International Journal of Machine Tools & Manufacture 49 (2009) 89–98

Contents lists available at ScienceDirect

International Journal of Machine Tools & Manufacture

journal homepage: www.elsevier.com/locate/ijmactool

Improving endmilling surface finish by workpiece rotation and adaptive toolpath spacing

Athulan Vijayaraghavan *, Aaron M. Hoover, Jeffrey Hartnett, David A. Dornfeld

University of California, 1115 Etcheverry Hall, Berkeley, CA 94720-1740, USA

ARTICLE INFO

Article history:
Received 9 March 2008
Received in revised form
15 July 2008
Accepted 21 July 2008
Available online 17 August 2008

Keywords:
Surface finish
Endmilling
Toolpath planning
Workpiece rotation
Adaptive path spacing

ABSTRACT

Free-form surfaces are being used in a growing number of engineering applications, especially in injection molding of consumer products. Decreasing the manufacturing cost and time of these molds will improve the efficiency of manufacturing injection molded consumer products. This paper is motivated by the need for simple strategies to improve the quality of and decrease the time required to machine free-form surfaces. We present two methods to improve the surface finish of parts finished with ball-nose endmilling. In the first method the surface finish is improved by finding an optimal orientation angle for the workpiece relative to the machining axis. In the second method finish is improved by adaptively varying the step-size when using raster toolpaths. The adaptive variation is controlled by a user-defined finish improvement factor, where the spacing density is increased only if the improvement in surface finish is greater than the finish improvement factor. These methods are implemented using an analytical model of the workpiece surface finish based on the mean scallop height of the machined surface. Results from the analytical model are verified with machining experiments, and we show that the adaptive spacing strategy can improve the surface quality by more than 50% with a small increase in the toolpath length. To achieve a similar improvement in surface quality by uniformly decreasing the path spacing results in a much larger increase in the toolpath length. The strategies discussed in this paper allow process planners intuitive control over the toolpath layout and spacing and improve the efficiency of machining high quality parts.

1. Introduction

The use of free-form surfaces in engineering applications has been growing in recent years, especially in manufacturing injection molds for consumer electronic parts. An increasing number of consumer electronic products are being designed with smooth ergonomic surfaces which are pleasing to touch. Since these parts are mostly manufactured using injection molding, it is very important that the injection molds are manufactured to very tight tolerances. A parallel trend seen in this industry is the shrinking of product life cycles. The time between successive design iterations is decreasing, and this requires product development and manufacturing to also be faster. Finally, market pressures are forcing manufacturers to continuously cut costs and increase the efficiency of the design and manufacturing phases. Given these driving forces, there is a need for innovative strategies to decrease the time and cost for manufacturing these products.

A large cost and time component in the development of injection molded parts is in machining the die itself, as the quality of plastic injection molded parts is directly related to the surface quality of the injection molds used in their manufacturing. Injection mold surfaces are usually finished with ball-nose endmilling operations to achieve a high quality surface finish. This is especially the case in contoured surfaces. Endmilling is also required when the molds are cast, as the finish from casting is usually not good enough for direct use in molding. In some cases for very precise molded parts, finishing operations are performed on the parts after they are molded. Developing ways to create mold surfaces smooth enough so that the parts produced need no post-processing after de-molding provides an enormous advantage to manufacturers because these steps can be time-consuming and expensive.

In this paper we present two methods to improve the surface finish of parts finished with ball-nose endmilling using raster toolpaths. In the first method, the surface finish is improved by finding the rotation angle for the workpiece relative to the machining axis which maximizes finish. In the second method, the surface finish is improved by adaptively varying the step size in the toolpath based on a user-defined toolpath improvement factor. In this scheme the spacing density is increased only if it

* Corresponding author. Tel.: +1 510 508 0560; fax: +1 510 643 0966.
E-mail addresses: athulan@berkeley.edu (A. Vijayaraghavan), ahoover@me.berkeley.edu (A.M. Hoover), j_hartnett@berkeley.edu (J. Hartnett), dornfeld@berkeley.edu (D.A. Dornfeld).

0890-6955/$ - see front matter © 2008 Elsevier Ltd. All rights reserved.
doi:10.1016/j.ijmachtools.2008.07.015

leads to an improvement in the local surface finish greater than the finish improvement factor. This allows process planners intuitive control over the toolpath layout and spacing. These methods are implemented using an analytical model of the workpiece surface finish based on the mean scallop height in the machined surface.

This paper is motivated by the need for simple strategies to improve free-form machined surfaces. While advanced toolpath generation algorithms for five-axis machining can be used to improve the surface finish, implementing these algorithms requires significant manufacturing hardware (in the form of machine tools and process tooling) [1]. The methods discussed in this paper are simple to apply, and improve the surface quality without a significant change in the overall machining process. For this reason we focus on three-axis milling which is one of the most common methods for machining free-form surfaces. The next section discusses the basics of endmilling and surface generation, along with a survey of related literature in the field.

2. Background and related work

2.1. Endmilling surface generation

The fundamental activity in a machining process is the removal of material from a blank to create a surface. The topography of the surface created can be described at macro- and microscales. The macroscale corresponds to the scale of the cutting tool itself, and features in this scale are generated by the geometry of the cutting tool as it removes material. For ball-nose endmilling, the feature of the cutting tool that creates the macroscale topography is the diameter of the ball-nose. Microscale topography is created by the surface profile of the cutting tool itself, the material properties and phases of the cutting tool and workpiece materials, as well as process dynamics and consumables. Cutting parameters such as the spindle RPM and the machining feed also affect the finish of a surface.

There are a variety of metrics which can be applied in estimating the finish of a machined surface. It is very important to choose a metric that is appropriate for the application of the surface, and that it can discern between the surface roughness, waviness, and form [2,3]. Jiang et al. [4,5] discuss at length past and current trends in surface metrology, highlighting the development of surface metrology techniques over the years. In this paper, we use the R_a, R_z, and R_{max} roughness parameters to experimentally measure the finish of the machined surfaces. These parameters denote, respectively, the average roughness, the average peak-valley roughness, and the maximum peak-valley roughness [6,7].

Altan et al. [8] presented a detailed review on the design and manufacturing of dies and molds, highlighting the state-of-the art in the field. Tonshoff and Hernandez-Camacho [9] discussed the machining of injection molds using three- and five-axis endmilling, noting the importance of taking the tool-workpiece engagement angle into account when setting the process parameters. The importance of choosing an appropriate tilt angle on the tool wear and the surface quality was also discussed. Engin and Altintas [10] presented a mathematical model for the most common helical endmills seen in industry, and predicted and measured the surface finish from using these mills. Mizugaki et al. [11,12] presented geometric methods to estimate the profile of the machined surface in ball-nose endmilling. The authors developed a generalized analytical model that took into account the tool-workpiece orientation angle, as well as the cutting path in predicting the profile of the machined surface. Liu et al. [13] used the solid geometry of endmilling cutters to predict the effect of cutter geometry and machining parameters on the quality of endmilled surfaces. The surface topography was predicted based on the geometry of the tool's cutting flutes, and good results were obtained when feed and speed were incorporated into the model. Ryu et al. [14] focused on surface generation when using flat endmills and presented a detailed model to predict the surface topography, taking into account the cutter geometry, the cutting conditions, and the tool deflection. Sriyotha et al. [15] performed simulations to predict surface topography and roughness as a function of machining parameters for finish-milled surfaces. The model formulation was very detailed, taking into account parameters such as tool runout and wear.

Chen et al. [16] discussed the modeling, simulation and verification of scallop formation in ball-endmilling, capturing the scallop geometry in the direction of feed and in the direction orthogonal to feed. They demonstrated that in cases of high speed machining (HSM), the scallops generated in the feed direction are as large—and in some cases larger—than those generated in the direction orthogonal to the feed. They also investigated changing the tool-axis inclination angle to reduce the scallop height, and observed that an angle of 10° was sufficient to improve the surface finish when using a variety of tool diameters. Aspinwall et al. [17] discussed in detail the influence of cutter orientation and workpiece angle on the finish of Inconel 718 surfaces. Improvements in tool life and surface finish were seen when the workpiece was tilted at 45° and a downward cutter orientation was used. These results demonstrated the close relationship between surface finish and the relative orientation of the tool and the workpiece. Indeed, changing the workpiece inclination for improving finish has long been used in the manufacture of injection molds [9].

In contrast to these detailed surface finish models, the model used in this work is very simple as we only intend to capture the effect of the workpiece orientation and the toolpath spacing on the finish of the surface. The aim of this paper is to identify simple strategies which yield a large improvement in the surface finish, and for this purpose our simple model is adequate. The more exhaustive surface generation models [13–15], while being more accurate, are computationally intensive and can be challenging to apply in real-time analysis and visualization. Past work on changing the tool-workpiece engagement angle [9,16,17] has focused on ensuring a constant chip load on the tool during machining. Our workpiece rotation method aims to find the best orientation to control the surface finish from a purely geometric perspective. This method can be combined with results from studies of the tool engagement angle to realize greater improvements in the endmilling process. The methods described in this study also have applications in the reverse engineering of complex surfaces, which focus on tracing the geometrical features of a physical model [18,19].

2.2. Endmilling toolpath planning

The toolpath in a machining process is the sequential array of positions the tool passes through as it removes material. Toolpaths are designed according to the geometry of the desired surface and to reduce machining form errors such as burrs. Several strategies can be employed in designing toolpaths for endmilling processes. One of the most popular strategies is raster toolpaths which traverse the surface in a series of parallel straight line cutting paths. Another strategy is contour toolpaths, which trace constant height contours of the surface.

Extensive work has been done by the machining research community on endmilling toolpath generation. Loney and Ozsoy [20] were among the first to discuss the NC machining of

free-form surfaces. The surfaces were described as bicubic patches and the step size between toolpaths was calculated as a function of local patch properties to ensure an acceptable surface finish. Austin et al. [21] compared several discretization strategies employed in the NC machining of NURBS surfaces and concluded that an algorithm based on parametric rectangular subdivision performed best. Sun et al. [22] presented work focused specifically on machining free-form surfaces and computing optimal decompositions of the tasks involved to minimize machining time within surface finish and tolerance constraints. Elber and Cohen [23] developed a method to generate toolpaths for free-form milling by extracting surface iso-parametric curves. Feng and Li [24] discussed a method to generate constant scallop height toolpaths for the endmilling of free-form surfaces. They took into account the step size of the toolpath as well as the feed and speed of the tool. Kim and Yang [25] discussed an offsetting scheme to create toolpaths for triangular workpiece meshes. Toolpaths were generated based on these offset surfaces and machining tests using these toolpaths confirmed their validity. Park [26] discussed a method for generating both contour and raster toolpaths based on mesh slicing. This method was based on algorithms that removed the invalid portions of the toolpaths created from the mesh slices. Both these methods applied discretized triangular meshes to generate the toolpath successfully. Wright et al. [27] presented an offsetting method and a toolpath generation scheme for endmilling of free-form surfaces. The toolpaths were generated based on the geometry of the cutting tool and the offset surface.

In this paper we employ raster toolpaths in machining the workpiece. While contour toolpaths are very effective in creating precise surfaces, their effectiveness is entirely dependent on the features of the surface being machined. If the contouring is done for the entire workpiece, the toolpaths are influenced by the dominant contour and can be suboptimal in other regions of the mesh. If surface decomposition is used to prevent this, the decision of where to subdivide the surface can strongly influence the resultant surface finish. Also, using multiple contour regions can result in bad toolpaths at the interface of the regions, leading to unappealing visual artifacts.

Raster toolpaths, on the other hand, are more robust and can be applied in generalized surfaces. They do not lead to imprecisions from the tool "turning" inside the workpiece and result in uniformly directed visual artifacts. Errors due to machine tool control and interpolation are also diminished with raster toolpaths as the machine tool is interpolating in only one axis at any point in time. Past research in high-speed cutting has shown that there is a difference in the commanded feed and the actual feed during cutting [28]. This discrepancy can be decreased by minimizing the axis interpolation during cutting, which is possible with raster toolpaths. Rangarajan et al. [29] also showed that the forces during cutting can be decreased by minimizing axis interpolation, which is another benefit of using raster toolpaths.

Rastering algorithms can also be developed independent of the geometric characteristics of the surface (which are usually extracted from the B-Spline or NURBS description of the surface), which make them more flexible to apply. Our algorithm is based entirely on the expected finish of the surface and not its geometric characteristics. The next section discusses the analytical formulation of the surface finish model used by the algorithm.

3. Analytical formulation

To develop toolpath planning algorithms, we first need an analytical measure of the finish of a machined surface for a given toolpath. In this section a simple numerical measure for surface finish is presented. This metric is very competent for injection molds as it is based on the height of the excess material present in the surface after machining, which is an indication of how much material needs to be removed in post-processing operations [30,31]. The metric is especially appropriate for raster toolpaths. It is important to note here that we use this metric only in our toolpath selection algorithm; this is not a replacement for any of the standard surface finish metrics, although it correlates with some of them.

3.1. Surface finish model

The surface finish metric is based on the mechanics of surface generation in endmilling. Macroscale features generated in endmilling can be modeled as scallops, which are the result of uneven material removal. Fig. 1 illustrates this phenomenon—the scallop height is a function of the endmill radius and the spacing between adjacent passes of the endmill (which is called the step-size). The scallop height is also a function of the inclination of the workpiece with respect to the tool axis and the orientation of the workpiece about the tool axis.

Scallop height can be calculated by solving for the intersection point of the profile of the cutting tool from two successive passes. In the simple case of a flat workpiece, the scallop height is the z-coordinate of the intersection point, as illustrated in Fig. 1. In the case of a surface with inclination of θ with respect to the x-axis and a toolpath which traverses across the workpiece at an angle ϕ (see Fig. 2), the scallop height is the minimum positive root of the following equation:

$$4h^2 + 4h\varepsilon \sin\theta_{\text{eff}} - 4r^2 \cos^2\theta_{\text{eff}} + \varepsilon^2 = 0 \quad (1)$$

where $\theta_{\text{eff}} = \sin^{-1}(\sin\theta\cos\phi)$, ε is the toolpath spacing (step-size), r is the cutter radius, and h is the scallop height for which we are solving. We thus have the scallop height as a function of the cutting tool radius, toolpath step size, workpiece orientation, and workpiece inclination. It is important to note here that the scallop height is not directly a function of the depth of cut. The scallop height will be smaller than the depth of cut as long as the depth of cut is larger than the toolpath spacing, which is a reasonable assumption. The net surface finish of a workpiece is calculated as the mean height of all the machining scallops.

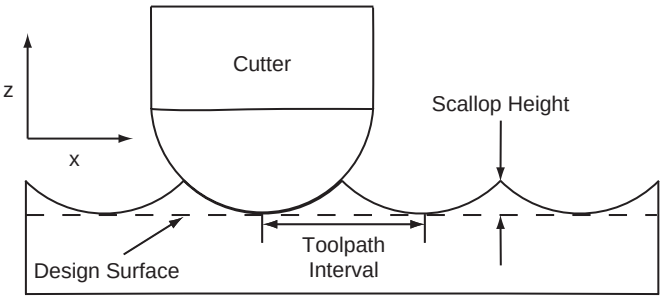

Fig. 1. Scallop geometry resulting from incomplete material removal.

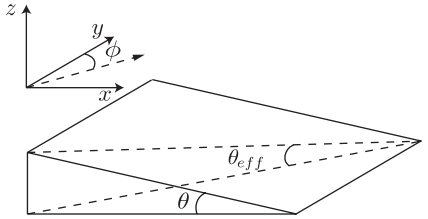

Fig. 2. Workpiece orientation to cutting tool.

Section 3.3 discusses how this metric is calculated for a specific workpiece.

3.2. Assumptions

This formulation only takes into account macroscale cutting phenomena and ignores the effect of dynamic phenomena. While cutting feed, chatter, machine tool vibration, cutting fluids, etc., affect the surface finish, this simple formulation is adequate to capture the effects of changing the machining toolpaths. The purpose of the metric is only to help in selecting machining toolpaths and not the machining parameters.

3.3. Applying the analytical model

The surface finish of a workpiece for a given toolpath orientation and spacing is calculated using a discretization of the workpiece surface. The workpiece surface is discretized at a finite density and is represented as a triangle mesh (a triangle mesh has the advantage of guaranteed planar faces). Since only raster toolpaths are used for the machining, the toolpaths can be mathematically represented as the intersection of the offset surface of the workpiece mesh (the offset-distance is the tool radius) by a family of parallel cutting planes, oriented at a fixed angle θ to the machining axes. To calculate the cutter line position, the mesh is intersected by the cutting planes. Intersecting a triangle with a plane yields either a point or a line-segment, and the intersection of the workpiece offset mesh with a plane yields a series of points and line-segments. The final toolpath consists of multiple such sets of points and line-segments. Fig. 3 shows a schematic of the plane-workpiece intersection.

With raster toolpaths the scallops occur regularly between adjacent cutting planes. For each pair of successive toolpath planes, a line of scallops occurring in all the triangles they pass through can be computed. Multiple scallops can pass through a single triangle in the mesh. Based on the height and length of the scallops in each triangle, a mean scallop height is calculated for each triangle. This quantity is the length-averaged scallop height of the triangle, and is calculated as follows. For a polygon k, which has m scallops each of length l_j, the mean scallop height, h_k is

$$h_k = \frac{\sum_{j=1}^{m} h_j l_j}{\sum_{j=1}^{m} l_j} \tag{2}$$

The net finish of a surface is calculated based on the mean scallop height of all the triangles in the mesh. The net finish is calculated as the area-averaged mean scallop height. Area averaging is used instead of triangle averaging to avoid over- or under-sampling regions of the mesh. The net finish F for a workpiece with n polygons, each of area A_i is calculated as

$$F = \frac{\sum_{i=1}^{n} A_i h_i}{\sum_{i=1}^{n} A_i} \tag{3}$$

This quantity is qualitatively comparable to the peak-to-valley surface roughness. Intuitively it denotes the average of the worst machining artifacts in the workpiece.

4. Implementation

This surface finish metric is calculated for the surfaces by representing them using simple triangular meshes. Triangular surface meshes have been extensively used in the literature, and a wide number of geometric algorithms have been implemented to operate on triangular and other polynomial meshes [32,33]. While generating the triangular meshes, however, care has been taken to ensure that the mesh discretization is sensitive to the local curvature in the mesh. The meshes used are suitably over-discretized in regions of high curvature and sparsely discretized in flat regions.

We use the OpenMesh geometric library for implementing the toolpath computations [32]. OpenMesh uses a half-edge data structure that makes it very efficient to process the meshes for toolpath intersections. A C++ program was used for all the calculations. The Coin libraries [34] were used to generate the mesh visualizations used in the paper.

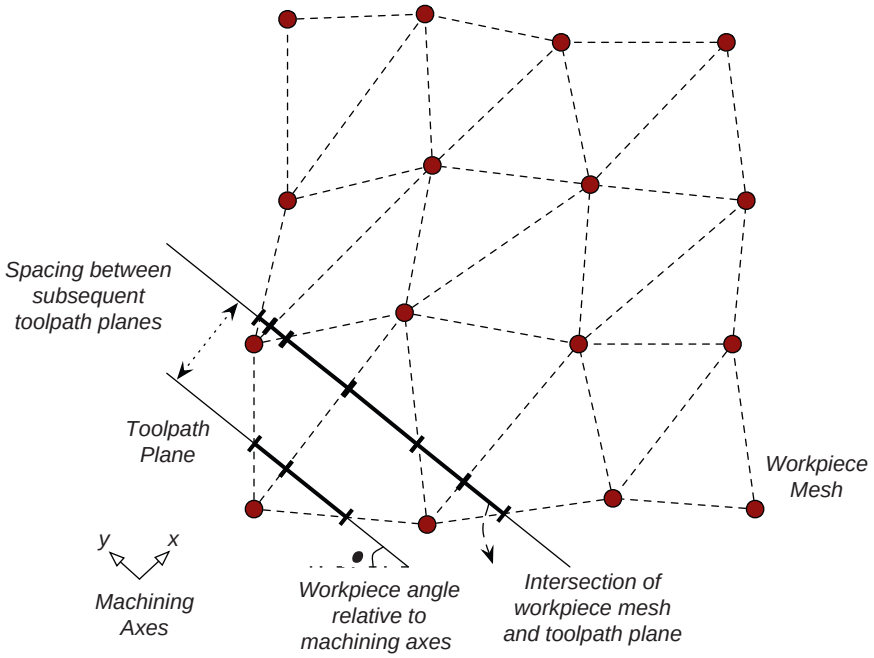

Fig. 3. Schematic of toolpath plane-workpiece intersection.

5. Improving surface finish by workpiece rotation

The analytical model discussed in Section 3 indicates the effect of the local orientation of the cutting tool relative to the workpiece in determining the surface finish. It is possible to obtain a better surface finish by controlling the local tool-workpiece orientation angle. In five-axis milling this can be achieved by changing the attack angle of the cutting tool [9]. But, with conventional three-axis milling the easiest way to achieve this is by manipulating the workpiece orientation angle.

Depending on the surface features, the surface finish from endmilling can be significantly improved by rotating the workpiece, while holding the other variables (tool radius, path spacing) constant. Using the surface finish model presented in Section 3 the surface finish was computed for the surfaces shown in Fig. 4. These are free-form surfaces with smooth variations of curvature. Wright et al. [27] employed a similar test surface for demonstrating their finish milling toolpath algorithm. The surfaces also do not demonstrate any obvious symmetry hinting at an "optimal" orientation angle.

Figs. 5–7 plot the relationship between surface finish and workpiece orientation for the test surfaces. The surface finish was calculated using the model discussed in Section 3, and the plots show surface finish variation for workpiece orientations between

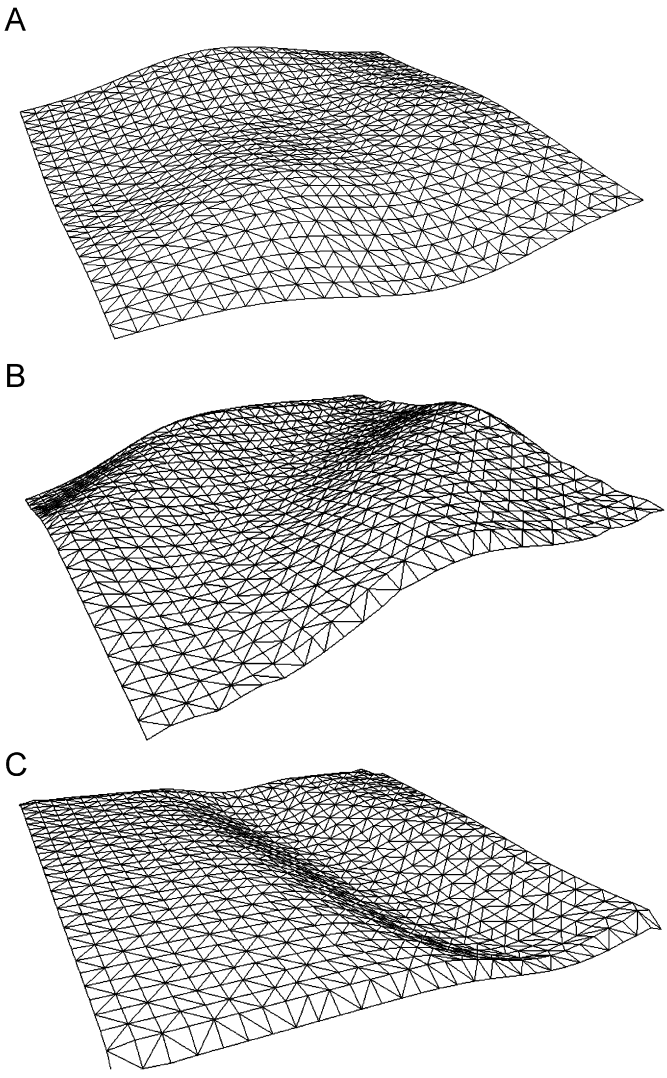

Fig. 4. Test surfaces used for analysis.

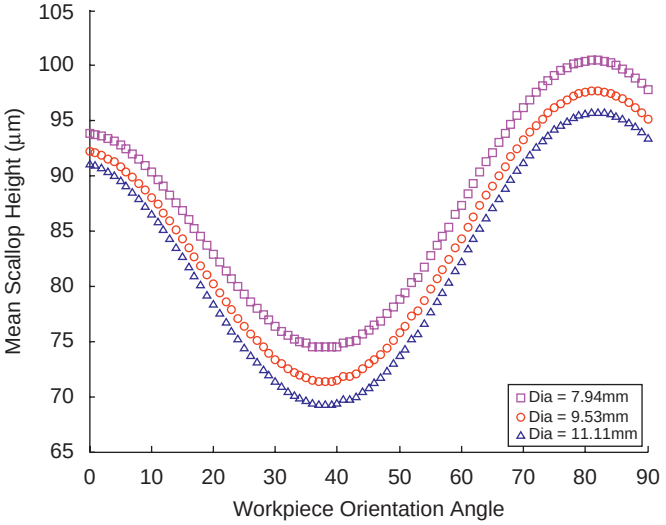

Fig. 5. Effect of workpiece orientation on surface finish of surface A (uniform path spacing: 0.047 mm).

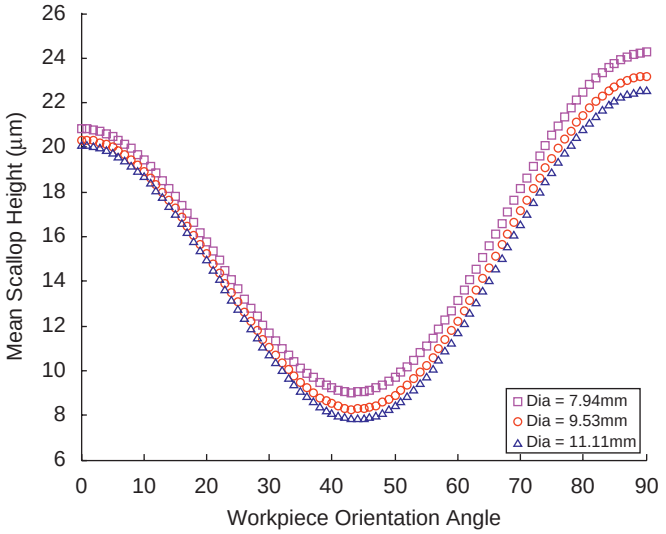

Fig. 6. Effect of workpiece orientation on surface finish of surface B (uniform path spacing: 0.047 mm).

0° and 90° in 1° increments using uniformly spaced raster toolpaths. The figures also show the effect of tool size on the finish at the different orientations. The plots indicate that the workpiece orientation has a strong impact on the finish of the workpiece. Table 1 lists the improvements in finish at the best case workpiece rotation angles. We can see that an improvement of at least 20% is seen in all the cases. At a fixed diameter, the toolpath length does not fluctuate significantly with the workpiece orientation as the spacing for all cases was held constant. Figs. 5–7 also show that the improvement from changing the workpiece orientation is vastly greater than what is possible by increasing the size of the tooling.

In certain cases the best orientation angle can be observed intuitively based on the surface features. For surface C, at the orientation of approximately 21° the toolpath lies parallel to the trough feature seen in the surface. Clearly this would maximize surface finish as it would minimize the gradient that the toolpath needs to traverse across, decreasing the mean scallop height in the machined surface. And correspondingly, for this surface the worst finish is at around 66°—which is 45° rotated away from the best

orientation—where the toolpath encounters the maximum surface gradient. Workpieces A and B do not suggest an obvious or intuitive toolpath orientation, and in these cases the numerical algorithm helps discover orientations which offer the greatest improvement in surface finish.

6. Strategies for adaptively spaced raster toolpaths

Another determinant of surface finish when using raster toolpaths is the spacing between adjacent toolpath lines. Indeed, the classic method to improve the surface finish for a workpiece is by decreasing the spacing between adjacent toolpath lines. While this method usually results in smoother surfaces, the gains in finish are accompanied by a corresponding increase in the toolpath length. Fig. 8 plots the effect of decreasing the path spacing on the finish and toolpath length for surface A. Decreasing the spacing results in a nonlinear increase in the length of the toolpaths. The challenge lies in improving the surface finish without an accompanied increase in toolpath length.

6.1. Strategy for adaptive toolpaths

An advantage of raster toolpaths is that it is possible to have very precise control over the density and spacing of the toolpaths in different regions of the workpiece. Much of the benefit of using raster toolpaths comes from this capacity of dynamic, local, refinement. As an illustration, consider the workpiece in Fig. 9. Three toolpath designs have been used to machine this workpiece, (a) shows a toolpath with wide spacing (b) shows a toolpath with very narrow spacing, and (c) shows a toolpath with non-uniform spacing. In (a) the toolpath is wide everywhere over the workpiece, which results in it missing some features. In (b) the toolpath is narrow, and while this ensures that it catches the steeper features, it is unnecessarily dense in the flatter areas of the workpiece where wide toolpaths are adequate—hence this toolpath has a high machining time. In (c) we strike a balance between these two cases, and the toolpath spacing is wide in the flatter regions and narrow in the regions with steeper features. Our objective is to develop an algorithm which can adaptively vary the path spacing without user intervention based on local surface features.

We use a novel adaptive toolpath strategy to generate toolpaths with locally varying path spacing. In this scheme, the toolpath density is locally increased only if the improvement in surface finish is greater than a user-defined threshold (the *finish improvement factor*). The algorithm is as follows:

(1) Create the starting toolpath-line at the zero position.
(2) Create the next toolpath-line at the default spacing.
(3) Compare the local finish at the current spacing to the local finish if the spacing is reduced by half.
(4) If the improvement in finish is greater than the finish improvement factor, accept the reduced spacing.
(5) Continue testing for a smaller finish until a pre-set minimum spacing is reached.
(6) Start again at the default spacing for the next toolpath line and continue the search.
(7) Sweep through the entire workpiece until the last toolpath-line is created.

The finish improvement factor (α) determines the minimum acceptable improvement in the surfaces. For example, if the

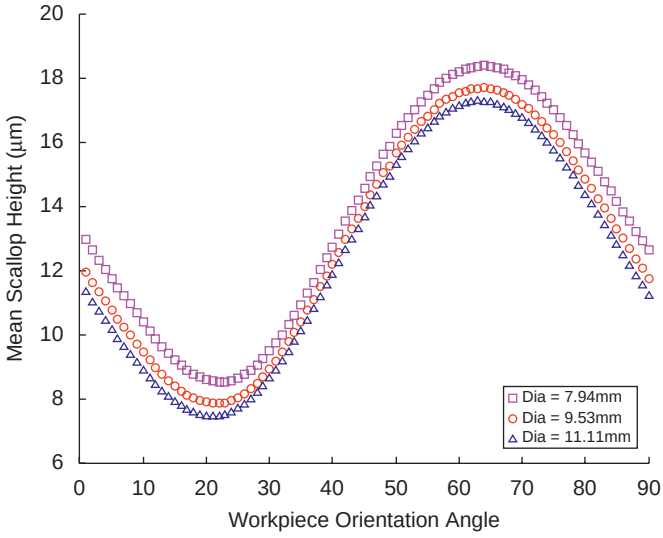

Fig. 7. Effect of workpiece orientation on surface finish of surface C (uniform path spacing: 0.047 mm).

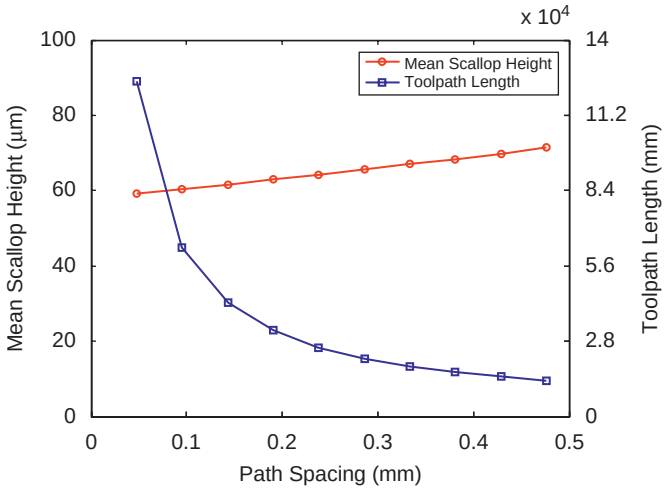

Fig. 8. Effect of path spacing on surface finish and toolpath length for surface A (tool diameter—9.53 mm).

Table 1
Improvement in finish from workpiece rotation

Workpiece	Dia: 7.94 mm		Dia: 9.53 mm		Dia: 11.11 mm	
	Angle (°)	Improvement (%)	Angle (°)	Improvement (%)	Angle (°)	Improvement (%)
A	39	20	39	23	38	24
B	43	57	43	59	43	61
C	22	36	21	36	21	36

'Angle' denotes the workpiece orientation angle with best finish (smallest mean scallop height).

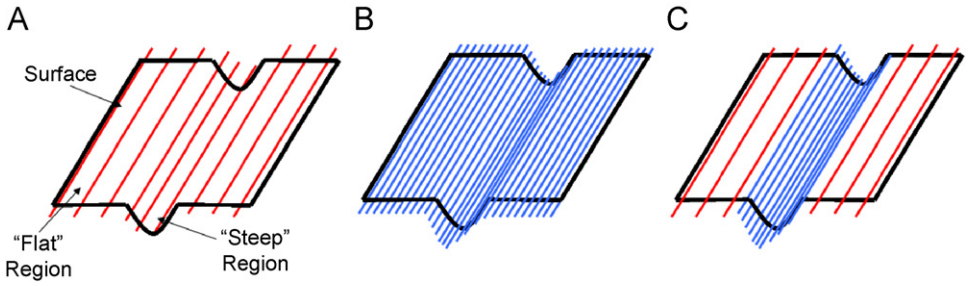

Fig. 9. Uniform and non-uniform spaced toolpaths.

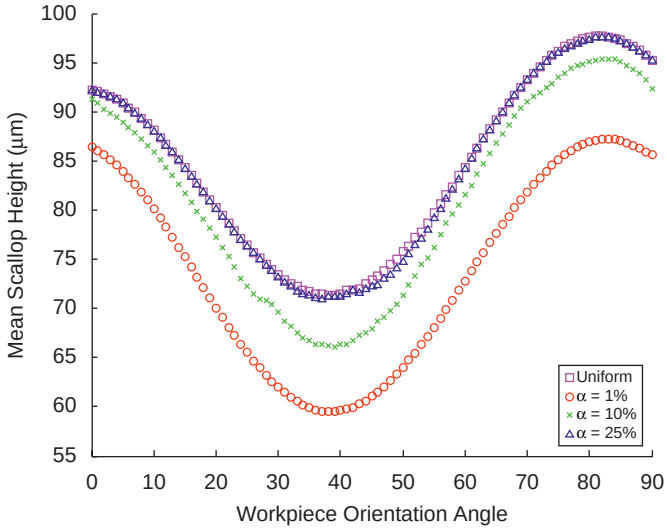

Fig. 10. Comparing uniform and adaptive spacing for workpiece A at varying orientation (tool diameter: 9.53 mm).

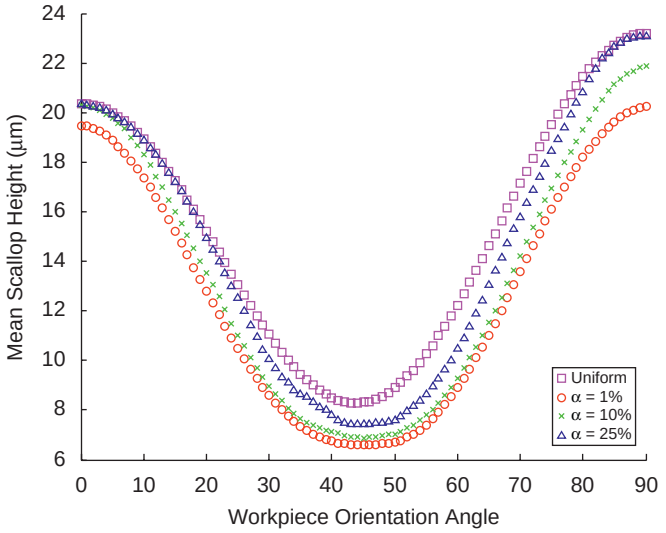

Fig. 11. Comparing uniform and adaptive spacing for workpiece B at varying orientation (tool diameter: 9.53 mm).

threshold is set at 10%, the toolpath spacing is locally halved only if at least a 10% improvement is seen in the local finish. This way, we avoid needlessly increasing the toolpath density in areas where no improvement can be seen. This algorithm allows the toolpath density to be increased only in regions where a significant benefit can be seen in the surface finish. The improvement threshold is determined based on the application and the surface finish requirements.

6.2. *Application of adaptive toolpaths*

The adaptive toolpath algorithm was applied in generating toolpaths for the surfaces shown in Fig. 4. Figs. 10–12 compare the finish at different orientations when using uniformly spaced toolpaths and adaptively spaced toolpaths with different finish improvement factors, α. The default path spacing for all these cases was 0.477 mm and the minimum spacing was 0.047 mm in the adaptive cases; a 9.53 mm diameter tool was used in all the cases. Table 2 lists the toolpath length for these cases at the best-case workpiece orientation, and the relative improvement in the finish from the adaptive toolpaths at different finish improvement factors. We can see that applying the adaptive spacing technique has the potential of improving surface finish by more than 10% over the gains possible by rotating the workpiece to the best-case orientation (from Table 1). The finish values shown in the tables and plots were calculated using the model outlined in Section 3. As expected, the improvement in surface finish with the adaptive toolpaths was greater at a lower improvement factor. At a high

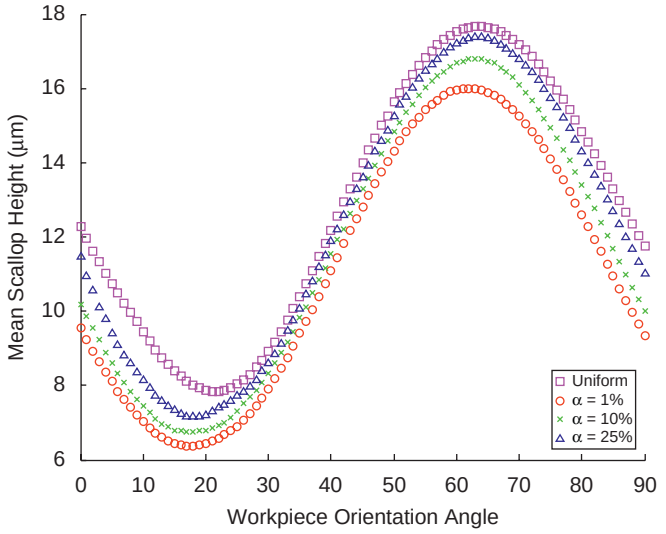

Fig. 12. Comparing uniform and adaptive spacing for workpiece C at varying orientation (tool diameter: 9.53 mm).

improvement factor, a larger improvement in finish is needed to increase the toolpath density. When the increase in finish is not possible, the toolpath density is not increased, and hence the cases with a high improvement factor have a similar finish and toolpath length to the uniform spacing cases. At a low improvement factor, a smaller improvement in finish is adequate to increase the toolpath density. Hence in these cases we see an

increase in finish accompanied by an increase in the toolpath length as well. It has to be noted that the increases in toolpath length in the adaptive cases are much smaller compared to uniformly decreasing the spacing to achieve the same finish (Fig. 8).

7. Experimental verification

The performance of the toolpath generation algorithm and surface finish model was verified experimentally by machining test surface A under multiple toolpath cases. Test surface A was very suitable for this as it was generated by convolving a series of gaussian functions over a square domain; it does not show any obvious planes of symmetry and has a high curvature variation over the domain. The surface was machined in Aluminum 6061-T6 using a Mori Seiki NV1500DCG three-axis mill. A 9.53 mm ball-nose Tungsten Carbide Cobalt (WC-Co) endmill was used for the process.

Workpieces were machined for the four toolpath cases shown in Table 3. An orientation angle of 39° was chosen as this was the angle with the greatest finish improvement when compared to the 0° orientation for surface A (from Table 1). Representative surface finish values for each workpiece were then measured using a MarSurf M1 Perthometer. Large undulations in the surface topography made it difficult to measure surface roughness over the entire workpiece with the Perthometer. Instead, we chose five representative regions on the part. Those regions included two different peak tops near the maximal surface height, steep faces on each of the two peaks, and one valley between peaks. At each region, we took measurements of R_a, R_z, and R_{max}, which are also summarized in Table 3. The machined test surface corresponding to Case 3 is shown in Fig. 13. Fig. 14 compares the surface finish and the toolpath lengths from the four cases.

We can see from the results that our proposed algorithm has the potential to provide a significant improvement in surface finish while also reducing machining time. Fig. 15 compares the improvements in surface finish from the experimental data in Cases 2 and 3 with the analytical model results in Table 2. By simply rotating the workpiece 39°, the R_z and R_a values are improved by 30% and 15%, respectively. Using the adaptive spacing algorithm, we were further able to improve R_z and R_a by over 25%, to a net improvement of 59% and 49%, respectively. These measurements compare very favorably with the model results. The improvement from the adaptively spaced toolpaths was accompanied by a comparatively small increase in the toolpath length. While the finish in Case 4 was the best, the toolpath was more than 6 times longer than the toolpath used in Case 3. It demonstrates that the surface finish can be improved only marginally if the spacing is decreased uniformly. In addition, the marginal increase comes at the added cost of a 10-fold increase in machining time over Case 1 and a sixfold increase over Case 3.

8. Conclusions

The workpiece orientation strategy has the potential to significantly improve the finish of free-form surfaces. While this

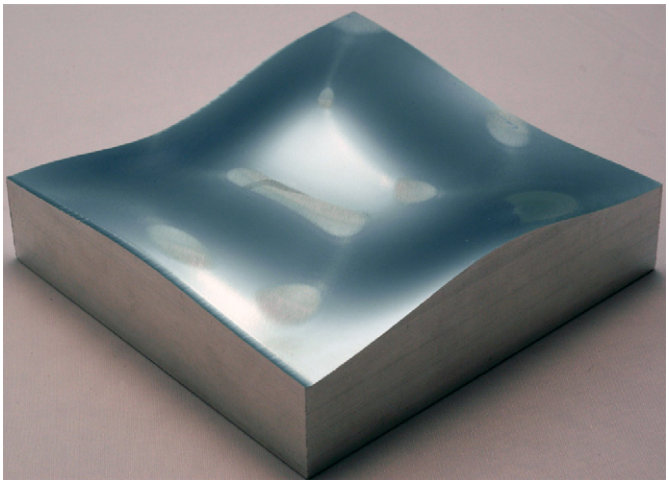

Fig. 13. Machined test surface for Case 3.

Table 2
Comparison of toolpath lengths for uniform and adaptive spacing (tool diameter: 9.53 mm)

Workpiece	Orientation (°)		Uniform	1%	10%	25%
A	39	Toolpath length	13 500 mm	99 000 mm	22 000 mm	12 500 mm
		Improvement in finish	23%	35%	28%	22%
B	43	Toolpath length	13 000 mm	58 000 mm	27 500 mm	16 500 mm
		Improvement in finish	59%	67%	66%	64%
C	21	Toolpath length	14 000 mm	65 500 mm	31 500 mm	24 000 mm
		Improvement in finish	36%	47%	44%	40%

Table 3
Experimental cases and roughness measurements

Case	Workpiece orientation (°)	Toolpath description	Toolpath length (mm)	R_a (μm)	R_z (μm)	R_{max} (μm)
1	0	Uniformly spaced at 0.477 mm	17 500	1.42	5.61	5.79
2	39	Uniformly spaced at 0.477 mm	13 500	0.99	4.75	5.69
3	39	Adaptively spaced. Maximum spacing = 0.477 mm, minimum spacing = 0.047 mm, $\alpha = 10\%$	22 000	0.58	2.87	3.91
4	39	Uniformly spaced at 0.047 mm	124 500	0.46	2.44	3.02

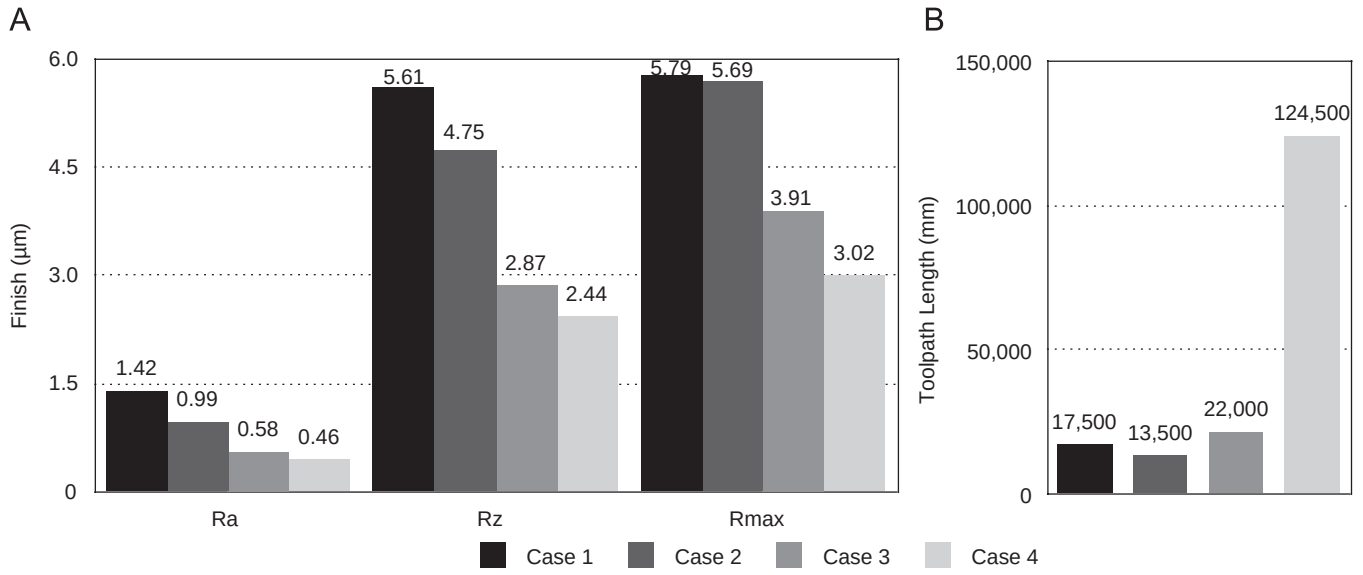

Fig. 14. (A) Surface finish measurements for the machining cases. (B) Toolpath length for the machining cases.

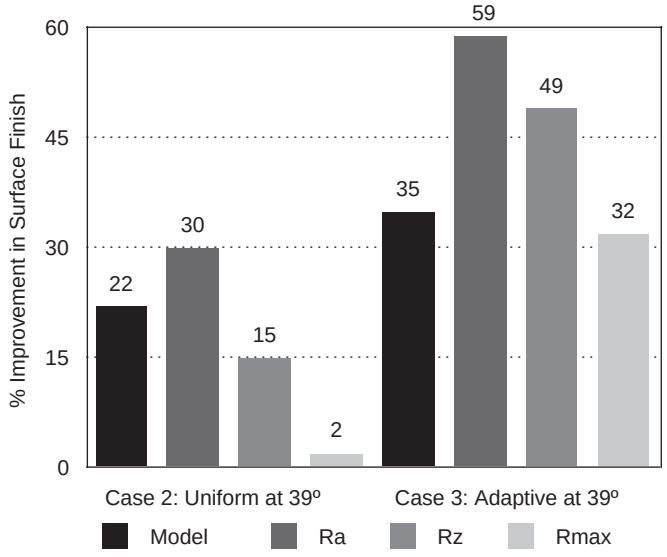

Fig. 15. Comparing improvements in surface finish from analytical results and experimental measurements. Improvements are calculated relative to the surface finish at 0° orientation and uniform path spacing (Case 1).

improvement may not be seen uniformly in all surfaces, our analytical model gives a quick way of estimating the surface finish at different orientations, simplifying the selection of a good orientation. The effectiveness of the analytical model in providing a qualitative measure of the best orientation was validated with the experimental data.

It was interesting to note that the orientation angle that produced the best surface finish remained more or less unchanged at different radii and under different adaptive and uniform spacing cases. This suggests that the orientation angle is a fundamental property of the surface for a given tool diameter. It would be very valuable to include this calculation in CAM packages—the optimal orientation angle can be quickly computed for a given free-form workpiece and used in all its path-planning. As this method does not call for a radical change in the toolpath layout, it can be implemented easily in a factory environment.

The adaptive toolpath strategy also helps in improving the finish without significantly increasing the machining time. Again, the analytical model was validated by the experimental data, and the model was capable of producing adaptively spaced toolpaths which improved the surface finish without a commensurate increase in machining time. Shorter toolpaths have the added advantage of reducing the machine tool power consumption, which further reduces the machining cost and improves the environmental sustainability of the machining process. Since the algorithm only increases the toolpath density in regions where an improvement is useful, the final toolpath reflects the *full potential* possible with the given tooling. For example, the algorithm may not decrease the spacing in a region with steep walls. This indicates that the decrease will not yield any improvement in the toolpath (for a given threshold) and that for a better finish perhaps a different orientation or a smaller diameter is needed. The algorithm combined with the workpiece orientation helps in fully spanning the possibilities for machining a workpiece for a given set of process tooling. This is important as in some production environments it may not be possible to have a wide range of tooling available.

The usefulness of our method can be improved by applying optimization tools to search for the best combination of process tooling, toolpath layout, and workpiece orientation angle for a given workpiece geometry. The method can be extended to adaptively change the machining parameters such as RPM and feed in real-time based on the local workpiece features. Techniques used in the reverse engineering of complex surfaces can also be applied in improving the accuracy of the analytical model with respect to experimental results [18,19].

The ultimate aim of this research is to develop tools which will allow product designers to quickly understand the effect of process planning choices. The surface finish metric in conjunction with the toolpath generation algorithm gives designers flexibility in selecting the best process plan for their application. These design tools help shorten the design-to-manufacturing pipeline and enable better integration of manufacturing planning with part design.

Acknowledgments

We thank D.E. Lee for his valuable comments and Bob Connors for helping with the measurements. We also thank the reviewers

for their valuable feedback. This research was supported by the Machine Tool Technology Research Foundation (MTTRF) and the industrial affiliates of the Laboratory for Manufacturing and Sustainability (http://lmas.berkeley.edu).

References

[1] M. Balasubramaniam, P. Laxmiprasad, S. Sarma, Z. Shaikh, Generating 5-axis nc roughing paths directly from a tesselated representation, Computer-Aided Design 32 (2000) 261–277.
[2] D.A. Dornfeld, D.E. Lee, Precision Manufacturing, first ed., Springer, Berlin, 2008.
[3] A. Tabenkin, Surface finish: a machinist's tool. A design necessity, MMS Online, 2008.
[4] X. Jiang, P.J. Scott, D.J. Whitehouse, L. Blunt, Paradigm shifts in surface metrology. Part I. Historical philosophy, Proceedings of the Royal Society A: Mathematical, Physical and Engineering Sciences 463 (2085) (2007) 2049–2070.
[5] X. Jiang, P.J. Scott, D.J. Whitehouse, L. Blunt, Paradigm shifts in surface metrology. Part II. The current shift, Proceedings of the Royal Society A: Mathematical, Physical and Engineering Sciences 463 (2085) (2007) 2071–2099.
[6] ISO 4287:1997, Geometrical product specifications (gps)—surface texture: profile method—terms, definitions and surface texture parameters.
[7] ASME B46.1-2002, Surface texture, surface roughness, waviness and lay.
[8] T. Altan, B. Lilly, Y.C. Yen, T. Altan, Manufacturing of dies and molds, CIRP Annals—Manufacturing Technology 50 (2) (2001) 404–422.
[9] H.K. Tonshoff, J. Hernandez-Camacho, Die manufacturing by 5- and 3-axes milling: influence of surface shape on cutting conditions, Journal of Mechanical Working Technology 20 (1989) 105–119.
[10] S. Engin, Y. Altintas, Mechanics and dynamics of general milling cutters. Part I: helical end mills, International Journal of Machine Tools and Manufacture 41 (2001) 2195–2212.
[11] Y. Mizugaki, M. Hao, K. Kikkawa, T. Nakagawa, Geometric generating mechanism of machined surface by ball-nosed end milling, CIRP Annals—Manufacturing Technology 50 (1) (2001) 69–72.
[12] Y. Mizugaki, K. Kikkawa, H. Terai, M. Hao, T. Sata, Theoretical estimation of machined surface profile based on cutting edge movement and tool orientation in ball-nosed end milling, CIRP Annals—Manufacturing Technology 52 (1) (2003) 49–52.
[13] N. Liu, M. Loftus, A. Whitten, Surface finish visualisation in high speed, ball nose milling applications, International Journal of Machine Tools and Manufacture 45 (10) (2005) 1152–1161.
[14] S.H. Ryu, D.K. Choi, C.N. Chu, Roughness and texture generation on end milled surfaces, International Journal of Machine Tools and Manufacture 46 (2006) 404–412.
[15] P. Sriyotha, A. Sahasrabudhe, K. Yamazaki, M. Mori, Geometrical modelling of a ball-end finish milling process for a surface finish, Proceedings of the I MECH E Part B. Journal of Engineering Manufacture 220 (4) (2006) 467–477.
[16] J.-S. Chen, Y.-K. Huang, M.-S. Chen, A study of the surface scallop generating mechanism in the ball-end milling process, International Journal of Machine Tools and Manufacture 45 (2005) 1077–1084.
[17] D.K. Aspinwall, R.C. Dewes, E.G. Ng, C. Sage, S.L. Soo, The influence of cutter orientation and workpiece angle on machinability when high-speed milling Inconel 718 under finishing conditions, International Journal of Machine Tools and Manufacture 47 (2007) 1839–1846.
[18] M. Galetto, E. Vezzetti, Reverse engineering of free-form surfaces: a methodology for threshold definition in selective sampling, International Journal of Machine Tools and Manufacture 46 (10) (2006) 1079–1086.
[19] A. Courtial, E. Vezzetti, New 3d segmentation approach for reverse engineering selective sampling acquisition, The International Journal of Advanced Manufacturing Technology 35 (9) (2008) 900–907.
[20] G. Loney, T. Ozsoy, Nc machining of free form surfaces, Computer-Aided Design 19 (2) (1987) 85–90.
[21] S. Austin, R. Jerard, R. Drysdale, Comparison of discretization algorithms for nurbs surfaces with application to numerically controlled machining, Computer-Aided Design 29 (1) (1997) 71–83.
[22] G. Sun, C. Sequin, P. Wright, Operation decomposition for freeform surface features in process planning, Computer-Aided Design 33 (9) (2001) 621–636.
[23] G. Elber, E. Cohen, Tool path generation for freeform surface models, in: SMA '93: Proceedings on the Second ACM Symposium on Solid Modeling and Applications, ACM, New York, NY, USA, 1993, pp. 419–428.
[24] H.-Y. Feng, H. Li, Constant scallop-height tool path generation for three-axis sculptured surface machining, Computer-Aided Design 34 (9) (2002) 647–654.
[25] S.-J. Kim, M.-Y. Yang, Triangular mesh offset for generalized cutter, Computer-Aided Design 37 (10) (2005) 999–1014.
[26] S. Park, Sculptured surface machining using triangular mesh slicing, Computer-Aided Design 36 (3) (2004) 279–288.
[27] P.K. Wright, D.A. Dornfeld, V. Sundararajan, D. Misra, Tool path generation for finish machining of freeform surfaces in the cybercut process planning pipeline, Transactions of NAMRI/SME 32 (2004) 159–166.
[28] A. Vijayaraghavan, W. Sobel, A. Fox, D.A. Dornfeld, P. Warndorf, Improving machine tool interoperability using standardized interface protocols: Mtconnect (tm), in: Proceedings of International Symposium on Flexible Automation, 2008.
[29] A. Rangarajan, D. Dornfeld, Efficient tool paths and part orientation for face milling, CIRP Annals—Manufacturing Technology 53 (1) (2004) 73–76.
[30] M. Boujelbene, A. Moisan, N. Tounsi, B. Brenier, Productivity enhancement in dies and molds manufacturing by the use of c1 continuous tool path, International Journal of Machine Tools and Manufacture 44 (2004) 101–107.
[31] L.N. Lopez de Lacalle, A. Lamikiz, J. Munoa, J.A. Sanchez, Quality improvement of ball-end milled sculptured surfaces by ball burnishing, International Journal of Machine Tools and Manufacture 45 (2005) 1659–1668.
[32] M. Botsch, S. Steinberg, S. Bischoff, L. Kobbelt, Openmesh—a generic and efficient polygon mesh data structure, 2002.
[33] CGAL, Computational geometry algorithms library, 2008.
[34] Coin, Coin 3d libraries, 2008.